crystals

MDPI

Article

Electrocaloric Effect in $(1-x)(0.8Na_{0.5}Bi_{0.5}TiO_3\text{-}0.2BaTiO_3)-xCaTiO_3$ Solid Solutions at High Electric Fields

Ojars Martins Eberlins, Eriks Birks, Maija Antonova, Maris Kundzins *, Maris Livins and Andris Sternberg

Institute of Solid State Physics, University of Latvia, Kengaraga 8, LV-1063 Riga, Latvia; Ojars-Martins.Eberlins@cfi.lu.lv (O.M.E.); eriks.birks@cfi.lu.lv (E.B.); maija.antonova@cfi.lu.lv (M.A.); maris.livins@cfi.lu.lv (M.L.); andris.sternbergs@cfi.lu.lv (A.S.)

* Correspondence: maris.kundzins@cfi.lu.lv

Abstract: Recently, promising results were obtained in studies of the electrocaloric effect in thin films. Therefore, research into this effect at high applied electric field values in bulk ferroelectrics is an important task for those scoping out materials that could be appropriate for cooling devices based on the electrocaloric effect. The present study addresses electrocaloric effect in $(1-x)(0.8Na_{1/2}Bi_{1/2}TiO_3\text{-}0.2BaTiO_3)-xCaTiO_3$ solid solutions by the direct method in electric fields ranging from 0 up to 100 kV/cm and at temperatures of up to 150 °C. The choice of $0.8Na_{1/2}Bi_{1/2}TiO_3\text{-}0.2BaTiO_3$ as the starting composition is motivated by high spontaneous polarization within the studied range of electric fields, while $CaTiO_3$ is added to reduce depolarization temperature at, and below, room temperature. In the studied temperature range, the maximal value of electrocaloric effect with temperature change of ΔT = 1.0 °C was found in the composition with x = 0.050 at 100 °C, having significant contribution from the entropy jump at the first-order phase transition induced by an electric field. At increasing $CaTiO_3$ concentration, the attainable ΔT decreases. Measurements of polarization current, which were taken simultaneously with ΔT measurements, allowed us to study differences between ΔT obtained by the direct and the indirect methods.

Keywords: sodium bismuth titanate; solid solutions; electrocaloric effect; dielectric polarization; phase transitions; Maxwell relation

Citation: Eberlins, O.M.; Birks, E.; Antonova, M.; Kundzins, M.; Livins, M.; Sternberg, A. Electrocaloric Effect in $(1-x)(0.8Na_{0.5}Bi_{0.5}TiO_3\text{-}0.2BaTiO_3)-xCaTiO_3$ Solid Solutions at High Electric Fields. *Crystals* **2022**, *12*, 134. https://doi.org/10.3390/cryst12020134

Academic Editors: Alexei A. Bokov, Guisheng Xu and Yizheng Tang

Received: 14 December 2021
Accepted: 16 January 2022
Published: 19 January 2022

1. Introduction

Recently, the electrocaloric effect (ECE) has attracted great interest, as it could be applied for designing active cooling elements, especially in micro and power electronics, and environmentally friendly air-conditioning and cooling systems. As a consequence, a large number of electrocaloric effect studies have been published (see a recent review by Barman et al. [1]). They bring a certain optimism regarding the prospect of implementation of electrocaloric cooling. First of all, it concerns ECE obtained in thin films. The promising results are obtained at high electric fields not suitable for bulk materials [2,3]. At the same time, the extremely small heat capacity of thin films significantly reduces practical application opportunities. Nevertheless, the possibility of such application is already demonstrated in PVDF thin film [4].

Regarding ECE in bulk ferroelectrics, two cases should be considered separately: (1) moderate electric fields and (2) high electric fields. In the easily accessible moderate electric field range (20–30 kV/cm), only a few compositions have been found with values of ECE temperature change ΔT exceeding 1 °C. All of these are related to entropy change at a first-order phase transition, which is induced by an electric field. One of these compositions is $Pb_{0.99}Nb_{0.02}(Zr_{0.70}Sn_{0.20}Ti_{0.05})_{0.98}O_3$, which belongs to $Pb(Sn,Zr,Ti)O_3$ solid solutions and has the largest values of ΔT found until now in this electric field range (2.6 °C at 30 kV/cm) [5]. It is established that the reason for such high ΔT values is the electric field-induced phase transition between ferroelectric and paraelectric states around 160 °C. Values

of ΔT at the first-order phase transition between ferroelectric and antiferroelectric states, observed for this composition at lower temperatures, as well as for other $Pb(Sn,Zr,Ti)O_3$ compositions, are much lower [6,7]. Unfortunately, the temperature region of the most expressed ECE in this case is not appropriate for cooling devices. $PbSc_{1/2}Ta_{1/2}O_3$ (PST)-based compositions are much more promising from this point of view. It is found that, at the first-order phase transition between ferroelectric and paraelectric states in partly B-site-ordered PST, observed in the temperature range from 0 to 10 °C, ΔT exceeds 1 °C at 20 kV/cm [8]. Later, increased B-site ordering and modification of PST with Sb allowed a ΔT increase of up to 1.5–1.8 °C at 25 kV/cm [9,10]. Still, this value is below the level necessary for implementing a promising prototype, which goes beyond mere demonstration of the working principle. At the moment, it seems that there are no suggestions for seeking out new materials with higher values of ΔT in this electric field range.

Another way to increase ΔT is to apply higher electric fields. Indeed, in PST, at 50 kV/cm, ΔT reached 2.3 °C [9]. Promising values of ΔT even at higher electric fields, exceeding 100 kV/cm, were reported in recent years. This was achieved by reducing the sample thickness and creating multilayers. In such a case, the reduced thickness allows one to increase the applied electric field, while the multilayer structure compensates for reduced heat capacity of a thin single layer. In $0.9PbMg_{1/3}Nb_{2/3}O_3$-$0.1PbTiO_3$ ceramics at 160 kV/cm, ΔT reaches 3.5 °C [11]. In $Ba(Ti_{0.8}Zr_{0.2})O_3$ ceramics at 145 kV/cm, ΔT is 4 °C [12], while in a multilayer structure of the same composition, even ΔT of 6 °C was achieved at 150 kV/cm [13]. Taking into account the large passive heat capacity in multilayer structures, which does not contribute to ECE, but consumes part of the generated heat [14], such a high value of ΔT is surprising. ΔT of 4 °C is reported also in a $BaTiO_3$ multilayer structure, but at two very different applied electric field values—176 and 350 kV/cm [15,16]. In a PST multilayer structure, ΔT of 5.5 °C was observed at 290 kV/cm [14]. Lower values are obtained in $PbMg_{1/3}Nb_{2/3}O_3$—at 90 kV/cm, ΔT of 2.4 °C was reported by Rožič et al. [17], and only 1.5 °C in Peräntie et al. [18]. Such results bring optimism about increasing ΔT by increasing of applied electric field. Even though the obtained values of ΔT are remarkably lower compared with thin films, they are usually within a range useful for development of the first prototype coolers with real output power, assuming problems related with breakdown fields are resolved. Unfortunately, measurements of ΔT in bulk ceramics at high electric fields are published rarely. Moreover, sometimes they are not mutually consistent, which can be seen also from the results mentioned in the previous paragraph.

The experimental results described above are obtained via direct measurement of the temperature change created by ECE (heat flow measurements by adapted DSC are also used). As follows from a large number of published results, another method—the indirect approach—is even more widely used for the study of ECE. In this case, ΔT values are calculated using the Maxwell's relations from electric field-temperature dependences of polarization *P(E,T)*, which are extracted from experimentally measured polarization hysteresis loops. The great popularity of such an approach is understandable—the experimental part is much easier to implement. It is especially valuable for studies in thin films, where performing direct ECE measurements is extremely complicated. Promising values of ΔT, obtained by the indirect method in $PbZr_{0.95}Ti_{0.05}O_3$ thin film [19], alone started the "renaissance" in ECE research.

In $Na_1/2Bi_1/2TiO_3$ (NBT)-based materials, ΔT values above 1 °C, as calculated by an indirect method, are reported repeatedly, paying more attention to the morphotropic phase boundary of NBT–$BaTiO_3$ solid solutions. Controversial results are obtained in a pure $0.94NBT–0.06BaTiO_3$ composition: in [20], the minimum of temperature dependence of ΔT ($\Delta T = -2.3$ °C at 70 kV/cm) is found at 50 °C; starting at room temperature, only positive, monotonously increasing values of ΔT at higher temperatures were measured by Li et al. [21]. Modification of this composition by 0.5 wt% of La [22] facilitated improved ΔT ($\Delta T = -2.6$ °C at 50 kV/cm, 65 °C). A similar value in the same temperature range was obtained in $0.9NBT–0.1K_1/2Bi_1/2TiO_3$ [23]. ECE in NBT, doped with various lanthanides,

is surprisingly sensitive to the choice of doping element [24], in particular for doping with 2 mol% Gd—reaching ΔT = 1.8 °C (90 kV/cm, 150 °C). Positive and negative ECE was frequently reported in the same composition across different temperature ranges [20–22].

ΔT values obtained by a direct method are lower. Le Goupil and Alford [25] have observed ΔT = 1.5 °C at 70 kV/cm, 125 °C in a 0.94NBT–0.06$KNbO_3$ solid solution. A similar value was obtained at 100 °C in 0.94NBT–0.06BT, where 1.5 mol% Bi was replaced by Sm [26].

The correspondence between the direct and the indirect methods is discussed repeatedly. Sometimes both methods give comparable results [27–29], although sometimes obtained results are clearly different [29–31]; even the sign of ΔT may differ [30,32]. Nonegodicity [31] and the presence of polar nanoregions (PNRs) [29,33] are used to explain such nonconformance. Violation of conditions necessary to apply the Maxwell's relations due to polydomain state existing in the studied materials is also mentioned [30,34]. Usability of polarization data should be treated with extreme caution if they are extracted from polarization hysteresis loops in bipolar electric fields, because reorientation of domains is essential for this kind of loops. Polarization hysteresis loops in the ferroelectric state should be at least with well-expressed saturation of polarization, while in the nonpolar phase, they should have low contribution of dielectric losses. Ignoring these requirements yields disputable results, such as negative ECE, sometimes obtained in $Na_{1/2}Bi_{1/2}TiO_3$-based compositions [22,23,35,36], or physically unrealistically high values of ΔT [37].

Taking into account the above considerations, extending the range of ECE results obtained by the direct method across a higher range of electric fields is of great importance. The presented research reports on detailed studies of ECE temperature change ΔT in $(1-x)(0.8Na_{1/2}Bi_{1/2}TiO_3\text{-}0.2BaTiO_3)-xCaTiO_3$ ((1−x)(0.8NBT-0.2BT)−xCT) solid solutions in electric field range up to 100 kV/cm. The initial composition of this group—0.8NBT-0.2BT (x = 0.00)—is located in the tetragonal side from the morphotropic phase boundary in the phase diagram of NBT-BT solid solutions. This choice is motivated by well-expressed ferroelectric–nonferroelectric phase transition in this composition with the largest polarization and the highest jump of lattice parameter comparing to the whole NBT-BT concentration range [38]. $CaTiO_3$ was added in order to reduce the depolarization temperature and increase ΔT around and below room temperature, which is a relevant condition considering the application of ECE in cooling devices.

2. Materials and Methods

$(1-x)(0.8Na_{0.5}Bi_{0.5}TiO_3\text{-}0.2BaTiO_3)-xCaTiO_3$ ((1−x)(0.8NBT-0.2BT)−xCT) ceramics with various $CaTiO_3$ concentrations (x = 0.050, 0.075, 0.100, and 0.125) were prepared by solid-state reaction from chemical-grade oxides and carbonates: Bi_2O_3 (purity 99.9%), TiO_2 (99.8%), Na_2CO_3 (99%), $BaCO_3$ (≥99%), and $CaCO_3$ (≥99%). The two-stage calcination was performed for 2 h at temperatures 850 °C and 1000 °C. Sintering was carried out for 3 h at 1140–1200 °C depending on composition.

The crystal structures of the crushed ceramic samples were determined using a PANalytical X'Pert PRO X-ray diffractometer (Malvern Panalytical Ltd., Malvern, UK).

Weak-field dielectric permittivity measurements were performed in a temperature range from room temperature to above 400 °C in the frequency range from 130 Hz to 1 MHz, using an impedance analyzer HP precision LCR meter 4284A. Samples of the compositions x = 0.050 and x = 0.075 were poled at room temperature before measurements.

Direct measurements of ECE (Figure S1, Supplementary file) were taken in samples of two different thicknesses for each (1−x)(0.8NBT-0.2BT)−xCT composition: up to 70 kV/cm for samples 0.3 mm thick and up to 100 kV/cm for samples 0.2 mm thick. Silver electrodes were fired on the sample surfaces at temperatures 500–600 °C. Then, 15 s long electric field pulses of various amplitudes up to 2 kV were applied via high-voltage amplifier TREK 609E-6. Temperature change of the measured sample and polarization current were simultaneously measured by Keithley nanovoltmeter 2182A and Keithley picoampermeter 6485, accordingly. In order to perform the measurements of temperature

change, a thin copper–constantan thermocouple was glued with silver paste onto the sample surface, which was electrically grounded. For application of voltage to the sample, thin copper wires (0.08 mm diameter) were also glued onto the sample electrodes. The edges of each sample were covered with a breakdown-resistant acryl coating. This coating, together with the glued thermocouple and the wires used to apply an electric field, created passive thermal capacity. The impact of this thermal capacity was evaluated in two ways: (1) by calculating it from weight of the glue, wires, and lacquer, and (2) by comparing the measured temperature change ΔT values of the samples of different thicknesses (from 0.5 mm, with only minor influence of passive thermal capacity to 0.2 mm) with the same composition. It was found that the measured ΔT value of 0.3 mm thick samples is 23% lower, and 41% lower in for 0.2 mm samples—compared with the real temperature change caused by ECE. The shape of time dependence of the temperature change $\Delta T(t)$ was carefully followed for absence of narrow pulses induced by change of electric field. The measured $\Delta T(t)$ curves reflected slow thermal decay of temperature difference (Figure S2, Supplementary File), related to incomplete thermal isolation between the sample and the environment, without any additional features. During the measurements, electric field dependence of ΔT was measured at sequential electric field pulses at chosen temperatures. The temperature-dependent measurements were taken in a Delta 9023 chamber up to 150 °C.

Polarization hysteresis loops were measured by the Sawyer–Tower method at triangular pulses, with voltage $U(t)$ slope of 100 V/s. Temperature dependence of remnant polarization was determined by measuring static pyroelectric effect on heating for the samples previously poled at room temperature at E = 70 kV/cm.

3. Results and Discussion

The X-ray diffraction patterns of the studied (1−x)(0.8NBT-0.2BT)−xCT compositions confirm pure perovskite structure. Splitting of pseudocubic [200] maximum for the composition x = 0.050 at 2θ = 46° is seen, while at higher $CaTiO_3$ concentrations, no deviations from the cubic pattern were detected (Figure 1).

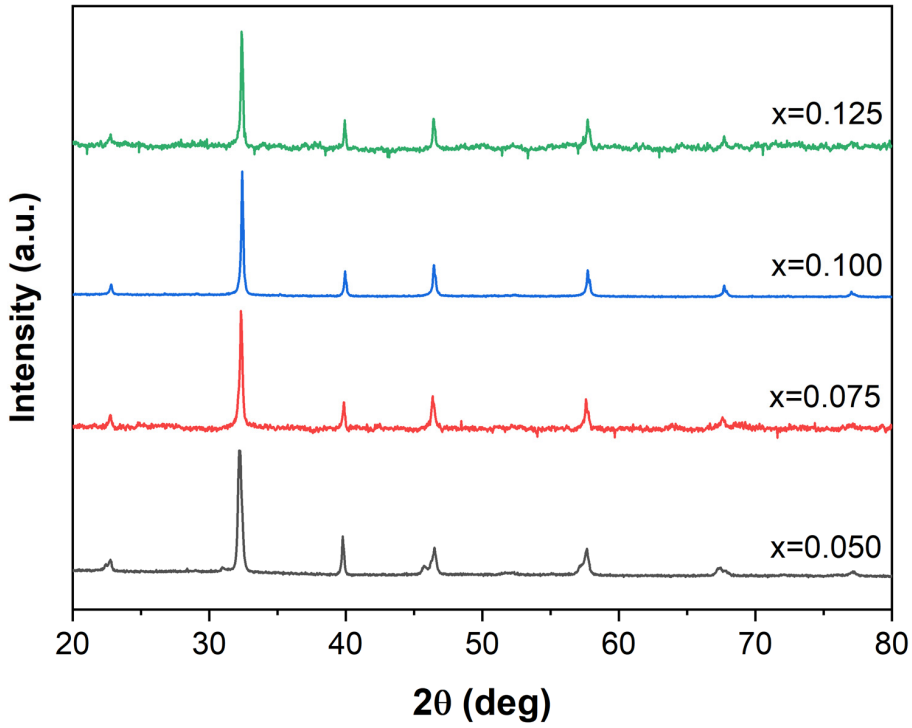

Figure 1. X-ray diffraction patterns at room temperature for (1−x)(0.8NBT-0.2BT)−xCT compositions with various concentrations.

Temperature dependences of the dielectric permittivity (ε) of dielectric losses ($tg\delta$) for all studied compositions are presented in Supplementary file, Figure S3, and reveal characteristics for NBT-based composition features: diffused frequency-independent maximum (for studied compositions located around 250 °C) and frequency-dependent shoulder at lower temperatures. Well-expressed, frequency-independent maximum in $tg\delta$ dependence on temperature of composition x = 0.05 slightly above 100 °C is related to depolarization temperature (T_d). For composition x = 0.075, corresponding anomaly is transformed into small jump close to 60 °C.

Polarization hysteresis loops for all studied compositions at bipolar electric field pulses at various temperatures are shown in Figure 2. Well-expressed double hysteresis loops for the compositions x = 0.050 and x = 0.075 are observed in the region of T_d. Signs of a double hysteresis loop at room temperature region are also observed for the composition x = 0.100, while $P(E)$ for the composition x = 0.125 is almost linear.

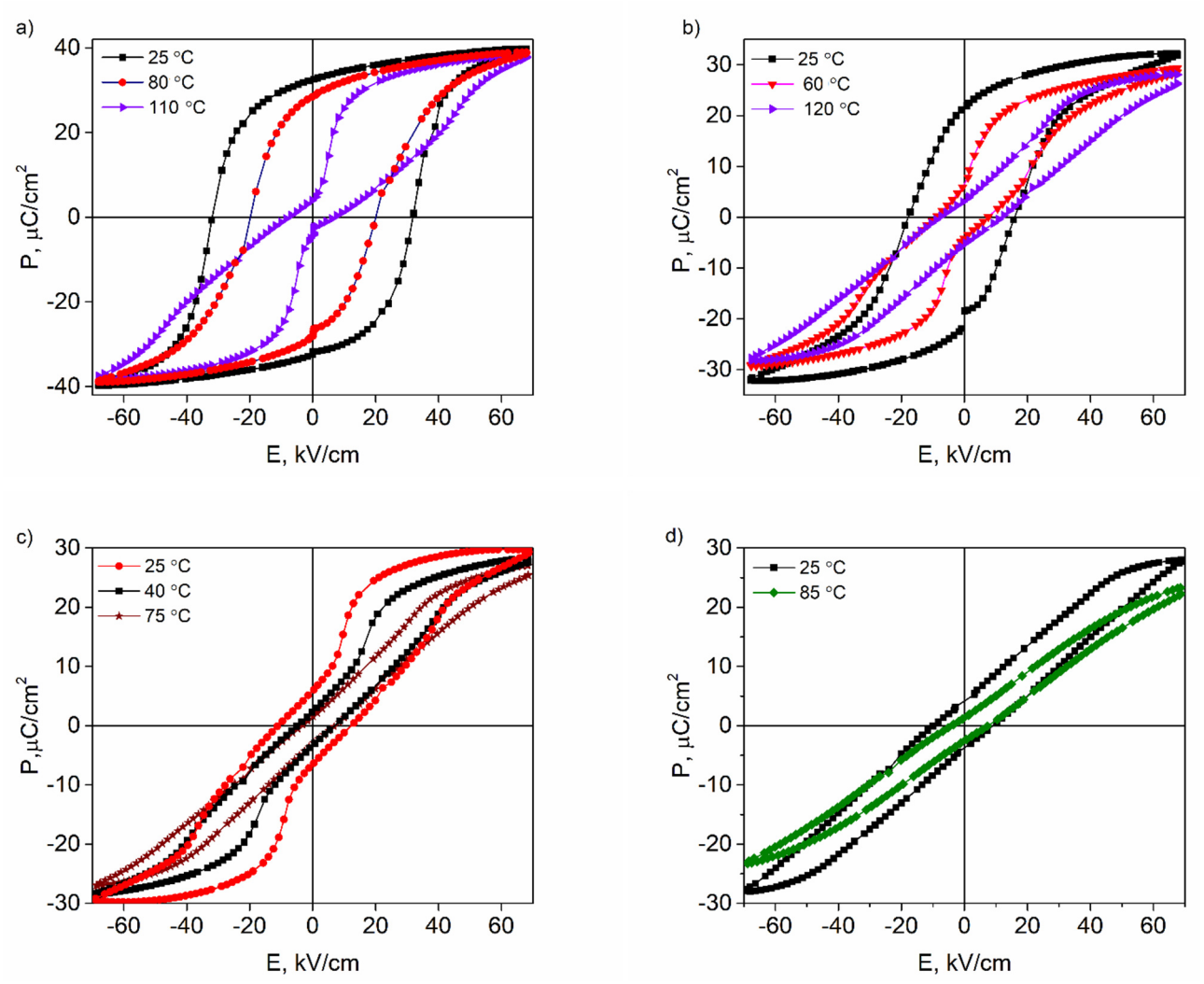

Figure 2. Polarization hysteresis loops at bipolar electric field pulses for (1−x)(0.8NBT-0.2BT)−xCT compositions x = 0.050 (**a**), x = 0.075 (**b**), x = 0.100 (**c**), and x = 0.125 (**d**) at various temperatures.

Temperature dependences of remnant polarization $P_{rem}(T)$ for the compositions which are in the ferroelectric phase at room temperature (x = 0.050, x = 0.075) are presented in Figure 3. The dependences were determined in two ways: (1) calculated from measurements of static pyroelectric effect, and (2) extracted from bipolar hysteresis loops at different temperatures. In both cases, $P_{rem}(T)$ decreases if temperature is increased, but, in the case of static pyroelectric effect, this dependence is more expressed. The abrupt drop of $P_{rem}(T)$

around 100 °C for the composition with x = 0.050 and around 40 °C for the composition with x = 0.075 indicates the region of depolarization temperature T_d.

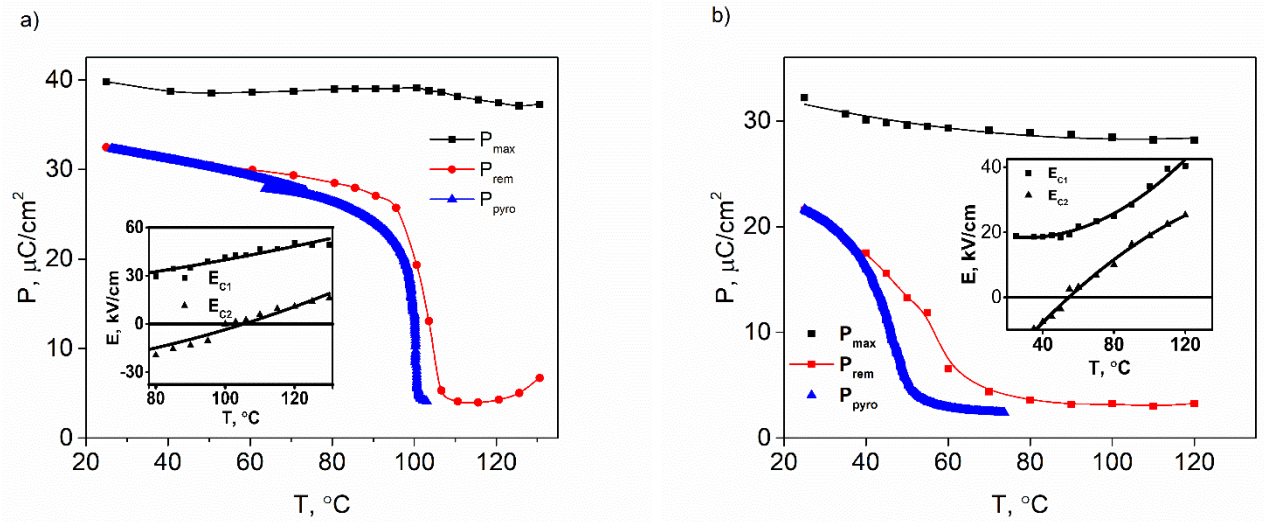

Figure 3. Temperature dependences of maximal (P_{max}) and remnant (P_{rem}) polarization for (1−x)(0.8NBT-0.2BT)−xCT compositions with x = 0.050 (**a**) and 0.075 (**b**), determined from polarization hysteresis loops, as well as from static pyroelectric effect measurements. Inset in (**a**): Temperature dependence of the critical electric fields for the composition with x = 0.050. Inset in (**b**): Temperature dependence of the critical electric fields for the composition with x = 0.075.

Double hysteresis loops for (1−x)(0.8NBT-0.2BT)−xCT compositions x = 0.050 and x = 0.075 allow us to determine the temperature dependence of the critical electric fields in these compositions (insets in Figure 3). For both compositions, temperature dependence of the critical electric field E_{c2}, corresponding to the phase transition from ferroelectric state to nonpolar state upon reducing the electric field, crosses the *x*-axis (E_{c2} = 0). This temperature indicates the temperature at which the poled state remains after electric field is switched off in the direction of low temperatures. Therefore, this is another way to determine the depolarization temperature T_d. For the composition with x = 0.050, T_d is 100 °C, while for the composition with x = 0.075, it is 50 °C. Temperature dependence of another critical electric field, E_{c1}—characterizing the phase transition from nonpolar to ferroelectric state upon increasing of field—is less expressed.

Temperature dependences of ΔT of all studied compositions at 100 kV/cm pulses are presented in Figure 4. The presented experimental data are measured upon switching off the electric field pulse in order to avoid contribution of the Joule heat in the measured ΔT, which appears at the highest electric fields and temperatures. The composition with x = 0.050 at room temperature is in ferroelectric state, which is the reason for ΔT being low. Significant increasing of $\Delta T(T)$ is observed around 100 °C, corresponding to the depolarization temperature, where a drop in remnant polarization occurs (Figure 2). The diffused jump of $\Delta T(T)$ in the temperature range between 70 and 130 °C is apparently related to a mixed ferroelectric–nonpolar state at E = 0 below 130 °C. With increasing temperature, concentration of the ferroelectric phase at E = 0 decreases. In the case of the composition with x = 0.075, the jump is shifted towards lower temperatures and is more pronounced. The broad maximum of $\Delta T(T)$ indicates that the applied electric fields are sufficient to induce ferroelectric state in a wide range of temperatures above T_d. In the compositions with higher concentrations of $CaTiO_3$, T_d is no longer found in the temperature range above room temperature, and ΔT only weakly depends on temperature, while ΔT values are significantly reduced.

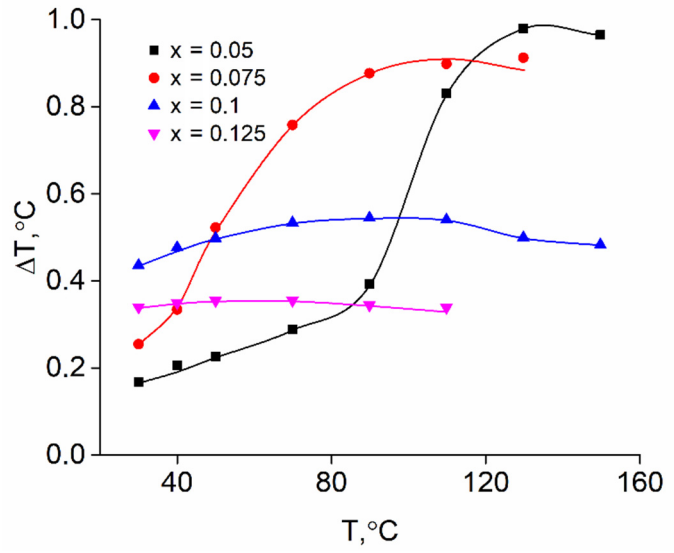

Figure 4. $\Delta T(T)$ for (1−x)(0.8NBT-0.2BT)−xCT with different concentrations, measured as a result of switching off electric field pulse E = 100 kV/cm.

Electric field dependences of ΔT for all studied compositions at different temperatures are shown in Figure 5. For the composition with x = 0.050 (Figure 5a), at measurement temperatures up to 90 °C, where the composition is in the ferroelectric state, ΔT is low across the whole electric field E range, with weakly negative curvature of $\Delta T(E)$. Above this temperature range, $\Delta T(E)$ contains significant contribution from the jump, which is observed in the vicinity of the critical electric field E_c and corresponds to the entropy jump (ΔS^{PT}) characteristic for the first-order phase transition:

$$\Delta T^{PT}(E_c) = \frac{T(E_c) \cdot \Delta S^{PT}}{c_{E_c}} \quad (1)$$

where c_{Ec} is heat capacity at the critical electric field. The ΔT^{PT} value, roughly evaluated from $\Delta T(E)$, is 0.65 °C. On the other hand, ΔT^{PT} can be evaluated indirectly from the Clausius–Clapeyron equation:

$$\Delta T^{PT} = \frac{T_c(E_c)}{c_{E_c}} \frac{dE_c}{dT} \cdot \Delta P \quad (2)$$

Considering that Equation (2) is derived from the condition that chemical potentials of both phases are equal, it does not take into account the actually-observed hysteresis of the critical electric field values upon increasing and decreasing the electric field (E_{c1} or E_{c2}—accordingly) due to metastability of both states. For this reason, temperature dependence of the critical electric field $E_c(T)$, which could be used in Equation (1), should have values between $E_{c1}(T)$ and $E_{c2}(T)$. In order to compare directly and indirectly determined values of ΔT^{PT} for the composition with x = 0.050, we have used the polarization jump at phase transition ΔP^{PT} and slopes of $E_{c1}(T)$ and $E_{c1}(T)$, as well as heat capacity of 0.92NBT–0.08BT at E = 0 [39], which should be close to the heat capacity of the measured compositions. Near the depolarization temperature, dE_{c1}/dT = 475 V/cm and dE_{c2}/dT = 775 V/cm. ΔT^{PT} calculated from these values is 1.3 and 2.2 °C accordingly—which is significantly higher than the directly measured value. The reason for such a difference could be the nature of the relaxor state existing in this case [38], which can be considered as a mixture of polar (polar nanoregions) and nonpolar phases instead of a pure nonpolar (paraelectric) phase.

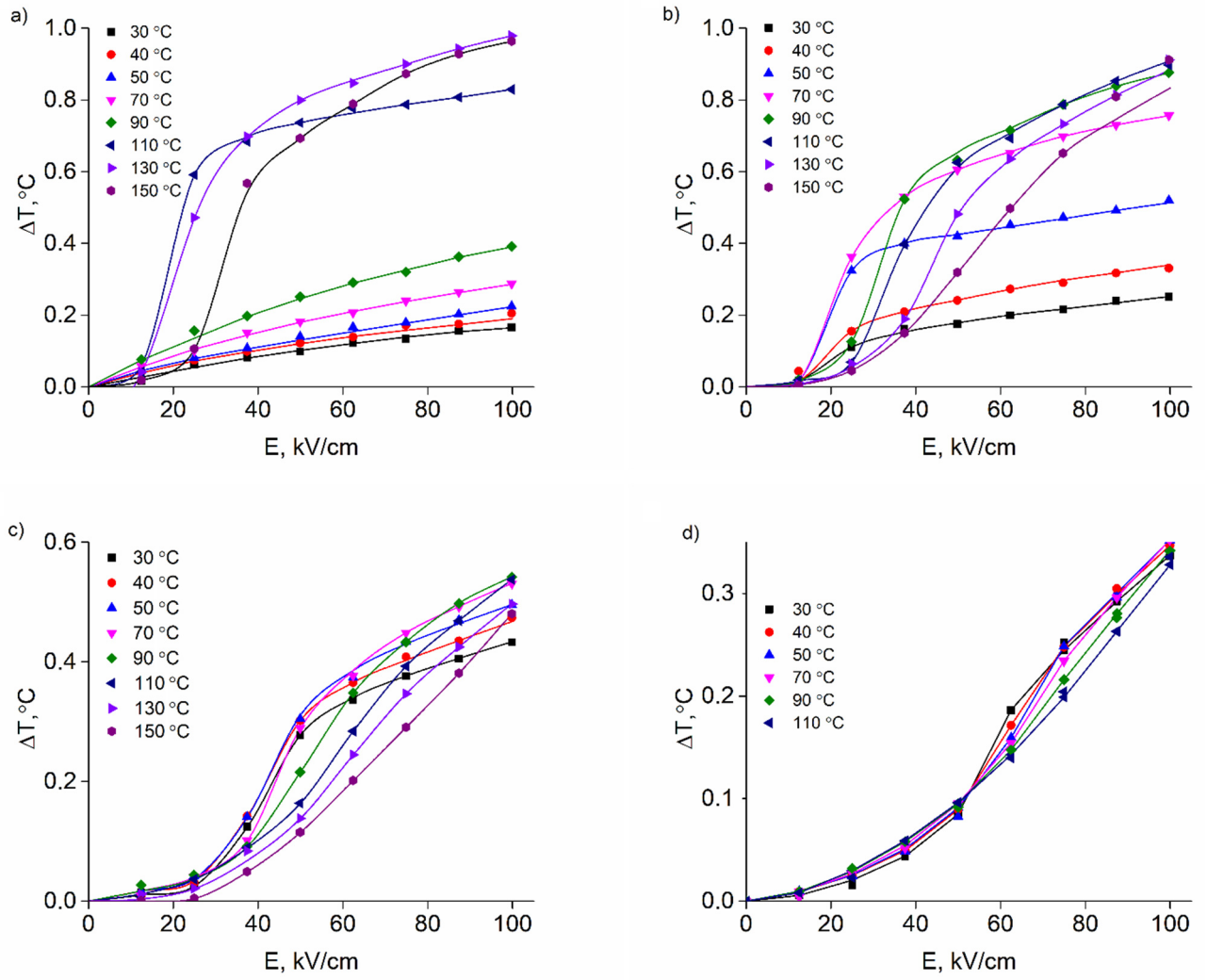

Figure 5. $\Delta T(E)$ for (1−x)(0.8NBT-0.2BT)−xCT compositions with x = 0.050 (**a**), x = 0.075 (**b**), x = 0.100 (**c**), and x = 0.125 (**d**), measured at different temperatures in the case when electric field pulse is switched off.

For the composition with x = 0.075, transformation of $\Delta T(E)$ with increasing or decreasing temperature (Figure 5b) follows the same trend as for the composition with x = 0.050. Obviously, due to lower T_d, related to the phase transition induced by the electric field, the jump of $\Delta T(E)$ is shifted towards lower temperatures, while the value of the jump is similar.

At higher temperatures, $\Delta T(E)$ for the compositions with x = 0.050 and x = 0.075 becomes diffuse, losing signs of electric field-induced first-order phase transition, and its values at maximal electric field pulses decrease significantly. At the same time, moderate increasing of ΔT due to the Joule heat, upon application of an electric field pulse, is observed.

$\Delta T(E)$ for the composition with x = 0.075 (Figure 5c) maintains the inflection point, presumably reflecting the diffuse transfer to the partly ferroelectric state, which almost disappears with increasing temperature. In the composition with x = 0.125, the inflection point disappears completely at higher temperatures (Figure 5d).

The difference between ΔT values with the electric field switched on and off is not related to Joule heat alone. This behavior is illustrated in the case of the composition with x = 0.075 at T = 40 °C (Figure 6a), where a significant difference between ΔT values appears already at moderate temperatures and electric fields. The reason for such a difference is slow relaxation of polarization observed in the unipolar $P(E)$ cycle (Figure 6b), which is

responsible for *P(E)* hysteresis and persists even after the cycle is finished and electric field reaches $E = 0$. Relaxation is complete within a few minutes and can be followed by measurement of polarization. However, the corresponding contribution to ΔT is outside the peak of $\Delta T(t)$, which is used to measure ΔT and is determined by thermal relaxation between the sample and thermocouple. This slow relaxation of polarization is very expressed in the temperature range where the electric field induced phase transition occurs.

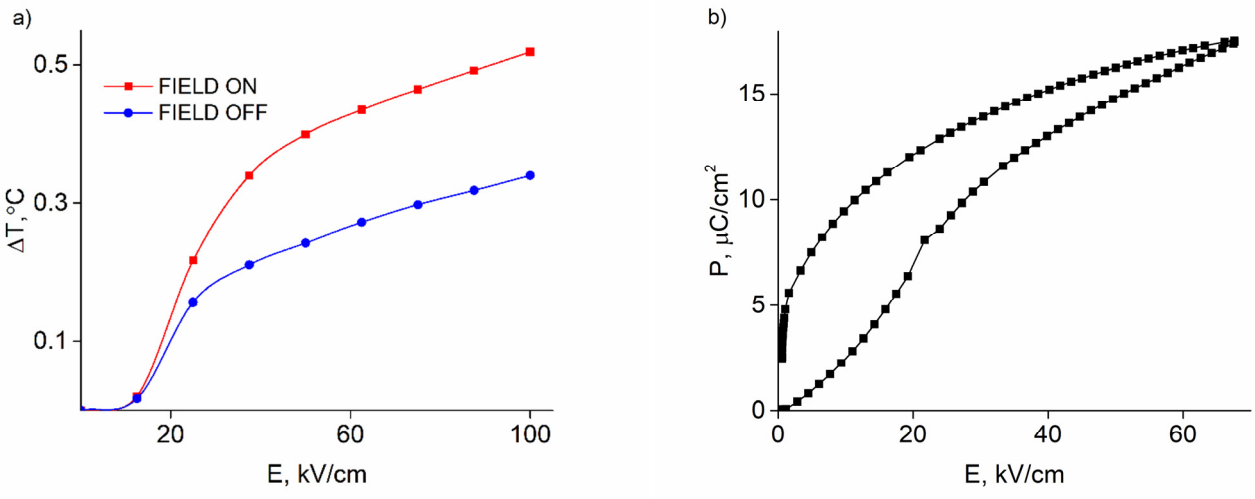

Figure 6. $\Delta T(E)$ (**a**) and $P(E)$ (**b**) for (1−x)(0.8NBT-0.2BT)−xCT composition with x = 0.075 at 40 °C ($P(E)$ is measured at $E = 67$ kV/cm unipolar pulse).

Experimentally measured polarization data are frequently used to determine ΔT by the Maxwell relation. In the ferroelectric state, data from the upper branch of bipolar hysteresis loops in the electric field ranging from the maximal value E_{max} to 0 are used for this purpose. Earlier, we noted that polarization, especially in the case of bipolar electric field pulses, depends significantly on ferroelectric domains switched by an electric field. Obviously, a switched domain pattern at different temperatures can be different, while polarization at fixed values of E (extracted from polarization hysteresis loops) upon change of temperature does not describe the continuous development of the same domain state. Especially in the case where E_{max} does not significantly exceed the coercive electric field, temperature dependence of concentration of switched domains is remarkably reduced comparing to the fully oriented case. As the coercive field usually decreases upon approaching the phase transition, concentration of the domains oriented in direction of electric field also increases. It can lead even to increased polarization upon increasing of temperature, which results in negative ECE, sometimes determined in NBT-based compositions by the indirect method [28–30]. At first sight, the problem with dependence of remnant polarization on domain switching can be avoided using measurements of static pyroelectric coefficient. However, unfortunately also in this case, contribution of domain reorientation or, more presumably, irreversible shift of domain boundaries contributes to polarization. These problems are illustrated in Figure 3. Temperature dependence of remnant polarization extracted from polarization hysteresis loops is more weakly expressed, compared with remnant polarization determined from measurements of static pyroelectric effect, and the corresponding T_d is shifted towards higher temperatures. At the same time, temporary change of direction of temperature for the composition with x = 0.050 around 50 °C (inset in Figure 2) clearly reveals irreversibility, related to irreversible domain processes. On the other hand, incomplete switching of domains, which should be quite a common behavior in polydomain ferroelectrics, reduces the value of ΔT compared with the fully aligned domain pattern. Therefore, both directly measured values—ΔT and $(\partial P/\partial T)_E$—can be far from thermodynamic conditions where direct and indirect values can be compared. Their coincidence in the ferroelectric state within the electric field range usually accessible

for bulk ferroelectrics (where contribution of domain processes is expected) could be rather accidental.

Outside of a stable ferroelectric state, polarization consists of solely electric field-induced polarization, and evaluation of ΔT from the Maxwell relation seems more appropriate. As unipolar pulses are used for measurements of ΔT, *P(E)* dependence could be also more adequate if measured at unipolar pulses. In the present case, the Maxwell relation will be applied to temperature dependence of polarization at different electric field values, obtained from measurements of polarization current at the same electric field pulses which were used in the measurements of ΔT (Figure 7).

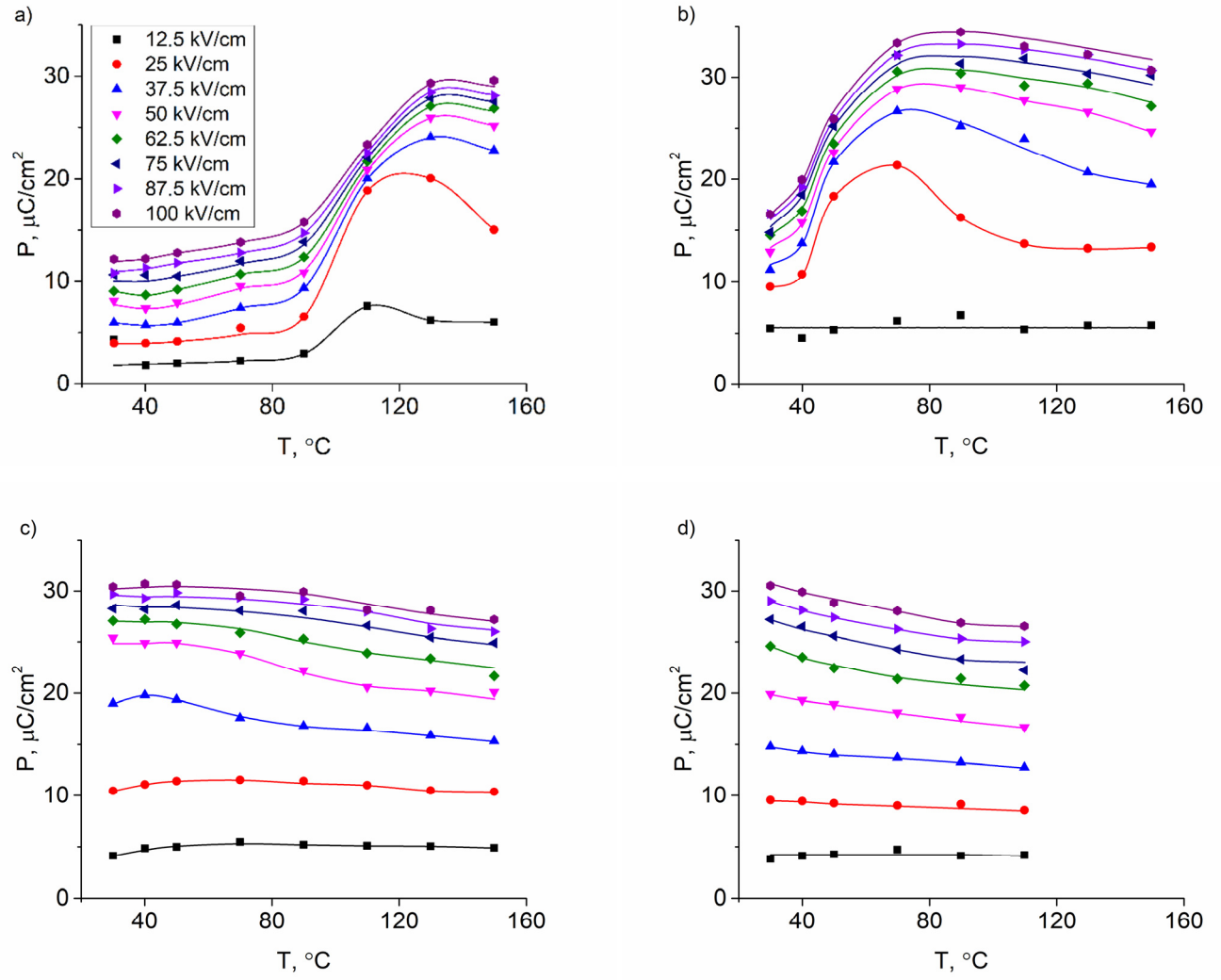

Figure 7. Temperature dependence of polarization at different electric fields for (1−x)(0.8NBT-0.2BT)−xCT compositions with x = 0.050 (**a**), x = 0.075 (**b**), x = 0.100 (**c**), and x = 0.125 (**d**), obtained from measurements of polarization current simultaneously with measurements of ΔT.

From our point of view, comparison of values of ΔT obtained by the direct and the indirect methods is not the best way, because integration of $(\partial P/\partial T)_E$ does not allow one to extract correspondence between both methods at different ranges of electric field. For that reason, differential layout of the Maxwell formula (Equation (1)) was transformed, allowing us to compare dT/dE and $(\partial P/\partial T)_E$.

$$\frac{dT}{dE} = -\frac{T}{c_E} \cdot \left(\frac{\partial P}{\partial T}\right)_E \quad (3)$$

As with the calculation of the jump of ΔT^{PT}, dependence of c_E on the electric field is neglected and values of heat capacity are borrowed from [39].

Examples of comparison of the results obtained by the direct and the indirect methods are presented in Figure 8. In the case where $\Delta T(E)$ has a clear enough inflection point, the shapes of curves representing the left and the right side of Equation (3) mutually correlate. However, the differences between these values can be significant. If the inflection point is not as pronounced (maximum of dT/dE as a function of E is low), even the shapes of the two curves do not correlate. This might partly be explained by rather flat $P(T)_E$ dependence in this case (low values of $(\partial P/\partial T)_E$ accordingly) when any additional contribution to polarization can seriously influence the values of $(\partial P/\partial T)_E$. From another point of view, as it was assumed above, the expressed inflection point could reflect at least a partial phase transition between nonpolar and ferroelectric phases, which could present a more appropriate case for using the Maxwell equation rather than rearrangement of polarization in the nonpolar phase clearly representing the relaxor state.

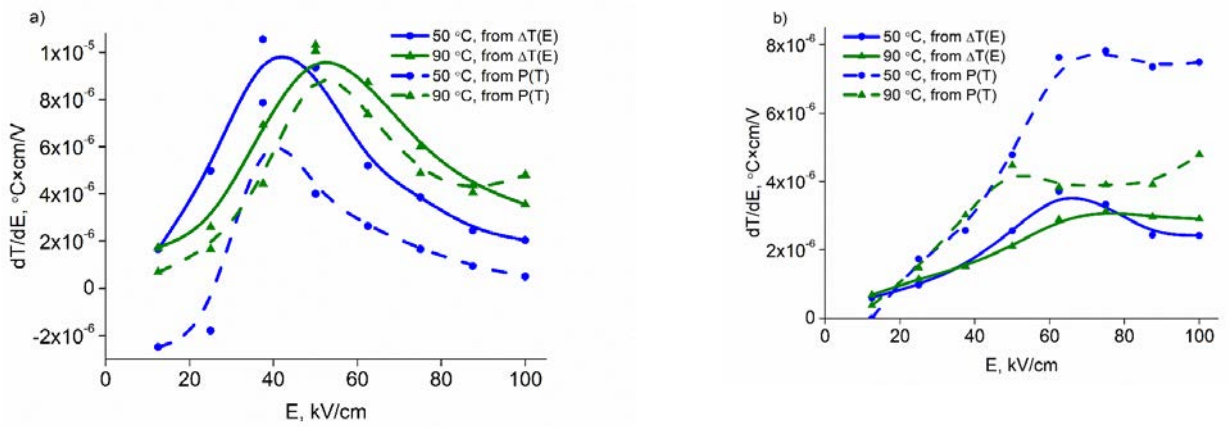

Figure 8. Comparison of dT/dE values obtained by the direct measurements of $\Delta T(E)$ and extracted from $P(T,E)$ according to Equation (3), using data from experimentally measured polarization current, for (1−x)(0.8NBT-0.2BT)−xCT compositions with x = 0.100 (**a**) and x = 0.125 (**b**).

4. Conclusions

The direct method is used for studies of electrocaloric effect in $(1-x)(0.8Na_{1/2}Bi_{1/2}TiO_3$-$0.2BaTiO_3)-xCaTiO_3$ solid solutions within the temperature range up to 150 °C at electric field pulses up to 100 kV/cm. The maximal values of ECE temperature change ΔT are found in the temperature region slightly above depolarization temperature. In the case of the composition with x = 0.050, ΔT reaches 1.0 °C at 100 °C. Approximately 0.65 °C in the total value of ΔT is accounted for by the contribution from the entropy jump at the phase transition between relaxor and ferroelectric states induced by an electric field. The directly measured temperature change is much lower compared with the temperature change calculated using the Clausius–Clapeyron equation. Such a difference is explained by the nature of relaxor state, which can be considered as a mixture of polar (polar nanoregions) and nonpolar phases instead of pure nonpolar (paraelectric) phase. In a wide temperature range around the depolarization temperature, values of ΔT measured upon switching off the electric field pulse are lower than the values obtained upon switching on the electric field pulse. The reason for the lower values is slow relaxation of polarization.

Increasing $CaTiO_3$ concentrations result in lower depolarization temperatures, but simultaneously significantly decrease the attainable values of ΔT.

In the temperature range above the depolarization temperature, a novel approach is used to compare the direct and indirect method of study of ECE. In the temperature range where the electric field at least partly induces a ferroelectric state, the shape of the calculated electric field dependence of the derivative dT/dE corresponds to the directly measured dependence, although the absolute values can differ substantially. Far above the depolarization temperature, correspondence between dT/dE obtained in both cases is lost.

Supplementary Materials: The following supporting information can be downloaded at: https://www.mdpi.com/article/10.3390/cryst12020134/s1, Figure S1: Principal diagram of experimental setup for measurements of ΔT and polarization current. Thermocouple is attached to two samples A and B. Samples are inserted in Delta chamber 9023 for measurements at different temperatures; HV—source of high voltage pulses TREK 609; nV—nanovoltmeter Keithley 2182A for measurement of ΔT; picoammeter Keithley 6485 for measurement of polarization current.; Figure S2: Example of dependence of temperature difference between sample and environment on time during measurement of ECE. Steep increasing and decreasing of $\Delta T(t)$ corresponds to switching on and off of field pulse, accordingly.; Figure S3: Temperature dependences of tdhe real part of dielectric permittivity (solid lines) at several frequencies (1 kHz, 20 kHz and 400 kHz) and of dielectric losses (dashed lines) on heating of all studied compositions of (1−x)(0.8NBT-0.2BT)-xCT: x = 0.050 (a), x = 0.075 (b), x = 0.100 (c) and x = 0.125 (d). Samples of compositions x = 0.050 and x = 0.075 were poled before measurements.

Author Contributions: Conceptualization, A.S. and E.B.; resources, E.B.; supervision, A.S.; methodology, O.M.E., E.B. and M.K.; validation, E.B.; investigation, O.M.E., M.A. and M.L.; writing—original draft, E.B.; writing—review and editing, M.K. and E.B., visualization, O.M.E. All authors have read and agreed to the published version of the manuscript.

Funding: This research was funded by the Latvian Science Council Fund, grant number lzp-2020/2-0080. The Institute of Solid State Physics, University of Latvia as the Center of Excellence has received funding from the European Union's Horizon 2020 Framework Programme, grant number 739508.

Data Availability Statement: The data presented in this study are available on request from the corresponding author.

Conflicts of Interest: The authors declare no conflict of interest.

References

1. Barman, A.; Kar-Narayan, S.; Mukherjee, D. Caloric effects in Perovskite Oxides. *Adv. Mater. Interfaces* **2019**, *6*, 1900291. [CrossRef]
2. Lu, S.G.; Rožič, B.; Zhang, Q.M.; Kutnjak, Z.; Xinyu, L.; Furman, E.; Gorny, L.J.; Lin, M.; Malič, B.; Kosec, M.; et al. Organic and inorganic relaxor ferroelectrics with giant electrocaloric effect. *Appl. Phys. Lett.* **2010**, *97*, 162904. [CrossRef]
3. Li, X.; Qian, X.-S.; Gu, H.; Chen, X.; Lu, S.G.; Lin, M.; Bateman, F.; Zhang, Q.M. Giant electrocaloric effect in ferroelectric poly(vinylidenefluoride-trifluoroethylene) copolymers near a first-order ferroelectric transition. *Appl. Phys. Lett.* **2012**, *101*, 132903. [CrossRef]
4. Ma, R.; Zhang, Z.; Tong, K.; Huber, D.; Kornbluh, R.; Ju, Y.S.; Pei, Q. Highly efficient electrocaloric cooling with electrostatic actuation. *Science* **2017**, *357*, 1130–1134. [CrossRef]
5. Tuttle, B.A.; Payne, D.A. The effects of microstructure on the electrocaloric properties of Pb(Zr,Sn,Ti)O_3 ceramics. *Ferroelectrics* **1981**, *37*, 603–606. [CrossRef]
6. Kabelka, H.; Fuith, A.; Birks, E.; Sternberg, A. Phase transitions of $Pb_{0.99}Nb_{0.02}(Zr_{0.75}Sn_{0.20}Ti_{0.05})O_3$ ceramics. *Ferroelectrics* **2001**, *258*, 61–70. [CrossRef]
7. Shebanov, L.; Kusnetsov, M.; Sternberg, A. Electric field induced antiferroelectric-to-ferroelectric phase transition in lead zirconate titanate stannate ceramics modified with lanthanum. *J. Appl. Phys.* **1994**, *76*, 4301–4304. [CrossRef]
8. Shebanov, L.; Birks, E.; Borman, K. The electrocaloric effect and characterization of structure of Pb(Sc1/2Nb1/2)O3 un $Pb(Sc_{1/2}Ta_{1/2})O_3$. *Fiz. Tverdogo Tela* **1988**, *30*, 2464–2469.
9. Shebanov, L.; Borman, K. On lead-scandium tantalate solid solutions with high electrocaloric effect. *Ferroelectrics* **1992**, *127*, 143–148. [CrossRef]
10. Shebanovs, L.; Borman, K.; Lawless, W.N.; Kalvane, A. Electrocaloric effect in some perovskite ferroelectric ceramics and multilayer capacitors. *Ferroelectrics* **2002**, *273*, 137–142. [CrossRef]
11. Vrabelj, M.; Uršič, H.; Kutnjak, Z.; Rožič, B.; Drnovšek, S.; Benčan, A.; Bobnar, V.; Fulanovič, L.; Malič, B. Large electrocaloric effect in grain-size-engineered $0.9Pb(Mg_{1/3}Nb_{2/3})O_3$–$0.1PbTiO_3$. *J. Eur. Ceram. Soc.* **2016**, *36*, 75–80. [CrossRef]
12. Qian, X.-S.; Ye, H.-J.; Zhang, Y.-T.; Gu, H.; Li, X.; Randall, C.A.; Zhang, Q.M. Giant Electrocaloric Response Over A Broad Temperature Range in Modified $BaTiO_3$ Ceramics. *Adv. Funct. Mater.* **2014**, *24*, 1300–1305. [CrossRef]
13. Ye, H.-J.; Qian, X.-S.; Jeong, D.-Y.; Zhang, S.; Zhou, Y.; Shao, W.-Z.; Zhen, L.; Zhang, Q.M. Giant electrocaloric effect in $BaZr_{0.2}Ti_{0.8}O_3$ thick film. *Appl. Phys. Lett.* **2014**, *105*, 152908. [CrossRef]
14. Nair, B.; Usui, T.; Crossley, S.; Kurdi, S.; Guzman-Verri, G.G.; Moya, X.; Hirose, S.; Mathur, N.D. Large electrocaloric effects in oxide mulilayer capacitors over a wide temperature range. *Nature* **2019**, *575*, 468–472. [CrossRef]
15. Bai, Y.; Zheng, G.-P.; Shi, S.-Q. Kinetic electrocaloric effect and giant net cooling of lead-free ferroelectric refrigerants. *J. Appl. Phys.* **2010**, *108*, 104102. [CrossRef]
16. Bai, Y.; Zheng, G.; Shi, S. Direct measurement of giant electrocaloric effect in $BaTiO_3$ multilayer thick film structure beyond theoretical prediction. *Appl. Phys. Lett.* **2010**, *96*, 192902. [CrossRef]

17. Rožič, B.; Malič, B.; Uršič, H.; Holc, J.; Kosec, M.; Kutnjak, Z. Direct Measurements of the Electrocaloric Effect in Bulk $PbMg_{1/3}Nb_{2/3}O_3$ (PMN) Ceramics. *Ferroelectrics* **2011**, *421*, 103–107. [CrossRef]
18. Peräntie, J.; Tailor, H.N.; Hagberg, J.; Jantunen, H.; Ye, Z.-G. Electrocaloric properties in relaxor ferroelectric $(1-x)Pb(Mg_{1/3}Nb_{2/3})O_3$–$xPbTiO_3$ system. *J. Appl. Phys.* **2013**, *114*, 174105. [CrossRef]
19. Mischenko, A.S.; Zhang, Q.; Scott, J.F.; Whatmore, R.W.; Mathur, N.D. Giant Electrocaloric Effect in Thin-Film $PbZr_{0.95}Ti_{0.05}O_3$. *Science* **2006**, *311*, 1270–1271. [CrossRef]
20. Uddin, S.; Zheng, G.-P.; Iqbal, Y.; Ubic, R.; Yang, J. Unification of the negative electrocaloric effect in $Bi_{1/2}Na_{1/2}TiO_3$-$BaTiO_3$ solid solutions by $Ba_{1/2}Sr_{1/2}TiO_3$ doping. *J. Appl. Phys.* **2013**, *114*, 213519. [CrossRef]
21. Li, L.; Xu, M.; Zhang, Q.; Chen, P.; Wang, N.; Xiong, D.; Peng, B.; Liu, L. Electrocaloric effect in La-doped BNT-6BT relaxor ferroelectric ceramics. *Ceram. Int.* **2018**, *44*, 343–350. [CrossRef]
22. Li, Q.; Wang, J.; Ma, L.; Fan, H.; Li, Z. Large electrocaloric effect in $(Bi_{0.5}Na_{0.5})_{0.94}$ $Ba_{0.06}TiO_3$ lead-free ferroelectric ceramics by La_2O_3 addition. *Mat. Res. Bull.* **2016**, *74*, 57–61. [CrossRef]
23. Wang, X.; Gao, H.; Hao, X.; Lou, X. Enhanced piezoelectric, electrocaloric and energy storage properties at high temperature in lead-free $Bi_{0.5}(Na_{1-x}K_x)_{0.5}TiO_3$ ceramics. *Ceram. Int.* **2019**, *45*, 4274–4282. [CrossRef]
24. Zannen, M.; Lahmar, A.; Asbani, B.; Khemakhem, H.; El Marssi, M.; Kutnjak, Z.; Es Souni, M. Electrocaloric effect and luminescence properties of lanthanide doped $(Na_{1/2}Bi_{1/2})TiO_3$ lead free materials. *Appl. Phys. Lett.* **2015**, *107*, 032905. [CrossRef]
25. Le Goupil, F.; Alford, N.M. Upper limit of the electrocaloric peak in lead-free ferroelectric relaxor ceramics. *APL Mater.* **2016**, *4*, 064104. [CrossRef]
26. Turki, O.; Slimani, A.; Seveyrat, L.; Sassi, Z.; Khemakhem, H.; Lebrun, L. Enhancement of dielectric, piezoelectric, ferroelectric, and electrocaloric properties in slightly doped $(Na_{0.5}Bi_{0.5})_{0.94}Ba_{0.06}TiO_3$ ceramic by samarium. *J. Appl. Phys.* **2019**, *125*, 174103. [CrossRef]
27. Le Goupil, F.; Berenov, A.; Axelsson, A.-K.; Valant, M.; Alford, N.M.c.N. Direct and indirect electrocaloric measurements on <001>-$PbMg_{1/3}Nb_{2/3}O_3$-$30PbTiO_3$ single crystals. *J. Appl. Phys.* **2012**, *111*, 124109. [CrossRef]
28. Fulanovič, L.; Drnovšek, S.; Uršič, H.; Vrabelj, M.; Kuščer, D.; Makarovič, K.; Bobnar, V.; Kutnjak, Z.; Malič, B. Multilayer $0.9Pb(Mg_{1/3}Nb_{2/3})O_3$–$0.1PbTiO_3$ elements for electrocaloric cooling. *J. Eur. Ceram. Soc.* **2017**, *37*, 599–603. [CrossRef]
29. Li, J.; Li, J.; Qin, S.; Su, X.; Qiao, L.; Wang, Y.; Lookman, T.; Bai, Y. Effects of Long- and Short-Range Ferroelectric Order on the Electrocaloric Effect in Relaxor Ferroelectric Ceramics. *Phys. Rev. Appl.* **2019**, *11*, 044032. [CrossRef]
30. Sanlialp, M.; Shvartsman, V.V.; Acosta, M.; Dkhil, B.; Lupascu, D.C. Strong electrocaloric effect in lead-free $0.65Ba(Zr_{0.2}Ti_{0.8})O_3$–$0.35(Ba_{0.7}Ca_{0.3})TiO_3$ ceramics obtained by direct measurements. *Appl. Phys. Lett.* **2015**, *106*, 062901. [CrossRef]
31. Lu, B.; Li, P.; Tang, Z.; Yao, Y.; Gao, X.; Kleemann, W.; Lu, S.-G. Large Electrocaloric Effect in Relaxor Ferroelectric and Antiferroelectric Lanthanum Doped Lead Zirconate Titanate Ceramics. *Sci. Rep.* **2017**, *7*, 45335. [CrossRef]
32. Turki, O.; Slimani, A.; Seveyrat, L.; Sebald, G.; Perrin, V.; Sassi, Z.; Khemakhem, H.; Lebrun, L. Structural, dielectric, ferroelectric, and electrocaloric properties of $2\%Gd_2O_3$ doping $(Na_{0.5}Bi_{0.5})_{0.94}Ba_{0.06}TiO_3$ ceramics. *J. Appl. Phys.* **2016**, *120*, 054102. [CrossRef]
33. Sanlialp, M.; Molin, C.; Shvartsman, V.V.; Gebhardt, S.; Lupascu, D.C. Modified Differential Scanning Calorimeter for Direct Electrocaloric Measurements. *IEEE Trans. Ultrason. Ferroelectr. Freq. Control* **2016**, *63*, 1690–1696. [CrossRef] [PubMed]
34. Birks, E.; Dunce, M.; Peräntie, J.; Hagberg, J.; Sternberg, A. Direct and indirect determination of electrocaloric effect in $Na_{0.5}Bi_{0.5}TiO_3$. *J. Appl. Phys.* **2017**, *121*, 224102. [CrossRef]
35. Cao, W.P.; Li, W.L.; Dai, X.F.; Zhang, T.D.; Sheng, J.; Hou, Y.F.; Fei, W.D. Large electrocaloric response and high energy-storage properties over a broad temperature range in lead-free NBT-ST ceramics. *J. Eur. Ceram. Soc* **2016**, *36*, 593–600. [CrossRef]
36. Kaur, S.; Arora, M.; Kumar, S.; Malhi, P.S.; Singh, M.; Singh, A. Abnormal electrocaloric effect near ambient temperature in MgO modified NBT-KBT. *Mater. Today Commun.* **2022**, *30*, 103028. [CrossRef]
37. Salea, A.; Chaipo, S.; Permana, A.A.; Jehlaeh, K.; Putson, C. The microstructure of negative electrocaloric Polyvinylidene fluoride-hexafluoropropylene copolymer on graphene loading for eco-friendlycooling technology. *J. Clean Prod.* **2020**, *251*, 119730. [CrossRef]
38. Dunce, M.; Birks, E.; Antonova, M.; Plaude, A.; Ignatans, R.; Sternberg, A. Structure and Dielectric Properties of $Na_{0.5}Bi_{0.5}TiO_3$-$BaTiO_3$ Solid Solutions. *Ferroelectrics* **2013**, *447*, 1–8. [CrossRef]
39. Bai, Y.; Zheng, G.-P.; Shi, S.-Q. Abnormal electrocaloric effect of $Na_{0.5}Bi_{0.5}TiO_3$-$BaTiO_3$ lead-free ferroelectric ceramics above room temperature. *Mat. Res. Bull.* **2011**, *46*, 1866–1869. [CrossRef]